Papers of Ship Research Institute Vol.32 No.2 Technical Report

A Simple Method to Remove the Boundary Layer on a Ground Plate

by

Andrew SOWDON*

Summary

This report summarizes the work to date on the removal of the boundary layer on a flat plate for use with Wing In Surface Effect Ship (WISES) model testing. A simple practical method is described which involves the use of a contraction and slot in order to suck the boundary layer from the plate. Theoretical aspects of the design are discussed with relation to the level of suction and the slot width. The boundary layer height was obtained through measurement of the mean velocity profile and a reduction of 50% was generally observed when suction was used. The effects on the forces on a low aspect-ratio wing were used to verify the technique for wing heights above 2.5% of the mean chord. Below this height separation of the boundary layer on the ground plate is thought to have altered the pressure distribution on the wing.

---

*Ship Performance Division

Received on March 2, 1995

Accepted on May 10, 1995

Contents

1. Introduction

The presence of a boundary layer when air is flowing over a solid surface is an accepted and expected phenomena and can be an integral and important part of the investigation. However, when referring to the real motion of a vehicle at low ground clearances in the absence of any atmospheric disturbances, there is generally no boundary layer on the ground. An accurate experimental representation of such a flow field in a wind tunnel is difficult for a number of reasons - a major one being the existence of the boundary layer on the surface representing the ground. This boundary layer can not be ignored in many applications including automobiles, racing vehicles and Wing in Surface Effect Ships (WISES), the latter of which is the concern of this report.

The exact extent to which the boundary layer (or lack of it) effects experimental results for WISES applications is not clear at present although in other fields it is widely recognized as a significant problem and strenuous efforts are made to remove it. However, for STOL and V/STOL craft it has been reported (T.R. Turner - 1966 [1]) that the presence of the boundary layer altered the measured lift coefficients on an aspect-ratio 6 model by 33% at a moderate ground height of 20% of the span (≡ 120% of the mean chord). The importance of such effects is clear when we consider that the static and dynamic stability of the craft is directly dependent upon the lift, drag and pitching moments.

Some recent WISES designs have used Power Augmented Ram (PAR) where the engine exhaust is directed under the wings. This provides additional lift during take off and allows slower and hence safer landing speeds. The effect of the boundary layer when PAR is used requires further examination.

1.1. Previous Methods for Simulating the Ground Plane

Previous studies have attempted to resolve the boundary layer problem in a number of ways, all of which involve either complex and expensive equipment or approximations to the flow field. These methods are summarised in Table 1 along with some comments and references. It is obvious that the moving belt technique provides the best simulation of the real flow field and is to be recommended for use where possible. However, the expense and complexity of the technique may be a limiting factor.

In order find the regions where the boundary layer has an effect T.R. Turner - 1966 [1] compared lift coefficients on a simple wing using a flat plate and a belt. The height where the methods started to disagree showed a linear correlation with lift coefficient according to Equation 1 indicating when to remove the boundary layer. M.C. Sullivan - 1978 [2] also analyzed the flow features in ground effect and came to a similar conclusion which included the effect of aspect ratio as given by Equation 2.

T.R. Turner - 1966 [1] also tested a tilt-rotor configuration where the majority of the lift originated from the power plants and not from aerodynamic factors. It was found that the belt was not required for

such cases. In the case of PAR the aerodynamic lift is greatly effected by the flow field from the power plants and hence the boundary layer should be removed if possible when indicated by Equation 2.

$$\frac{h/b}{C_L} < 0.05, \quad AR = 6 \tag{1}$$

$$\frac{h/b}{C_L} < \frac{1}{AR\ \pi} \tag{2}$$

where h is the wing height,* b is the span, C_L is the lift coefficient and AR is the aspect ratio.

Table 1 : Summary of Experimental Methods

Experimental Method.	Reported in;	Advantages	Disadvantages
Two identical models placed to form mirror images with the symmetry plane representing the ground.	M.P. Fink & J.L. Lastinger - 1961 [3]	Mean flow field is probably correct and good access for flow visualization. Simple apparatus.	Probably a non-zero vertical component of turbulence in the symmetry (ground) plane. Dynamic problems difficult to investigate. Added expense of making two models for each configuration. Smaller models required due to blockage effects. PAR effects difficult to simulate accurately.
As above but with a thin plate placed between the models just downstream of the leading edges where the pressure gradient is negative.	S. Katzoff & H.H. Sweberg -1941 [4]	As above plus the RMS flow field is better simulated. The boundary layer on the plate will be small and probably will not separate.	Dynamic problems difficult to investigate. Added expense of making two models for each configuration. Smaller models required due to blockage effects. PAR effects difficult to simulate accurately. Plate needs to be thin and correctly positioned which requires further experimental data.
Moving belt.	T.R. Turner - 1966 [1], T.R. Turner - 1967 [5]	Mean and RMS flow field are accurately simulated. Little or no increase in blockage. Works very well for high-lift configurations. Not overly sensitive to the belt speed so precise control is not required. Dynamic and PAR experiments possible.	Possibly expensive and complicated equipment. Upstream tunnel-floor boundary layer needs to be removed which adds expense and complexity, particularly for large wind-tunnels. Speed range limited to the operating range of the belt.

* The point from which this is measured is not clear and could effect the limit for small span craft and low heights.

2. Proposed Method

The method proposed in this report is cheap and easy to implement although there is possibly a small reduction in the size of models available for experimentation but this does not become a problem for the larger wind-tunnels for which this method was originally designed. The method is shown in Figure 1 and consists of a ground plate with a smoothed leading edge spanning the width of the wind tunnel and upon which the models will be tested.

The plate has a 45 degree slot cut across it at a convenient position downstream of the leading edge. This angle may not be the optimum but is a compromise between having a short length over which the suction pressure works (i.e. a higher angle), and a shallow rotation of the boundary layer into the slot (i.e. a lower angle). The plate is positioned above the tunnel floor in order to avoid the boundary layer on the floor and a smaller boundary layer grows on the ground plate which is more easily removed.

A contraction and expansion section (ramp) was fitted underneath the ground plate with the position of the maximum contraction being in line with the slot in the plate. The low pressure beneath the ground plate then sucks off the thin boundary layer on the upper surface of the plate.

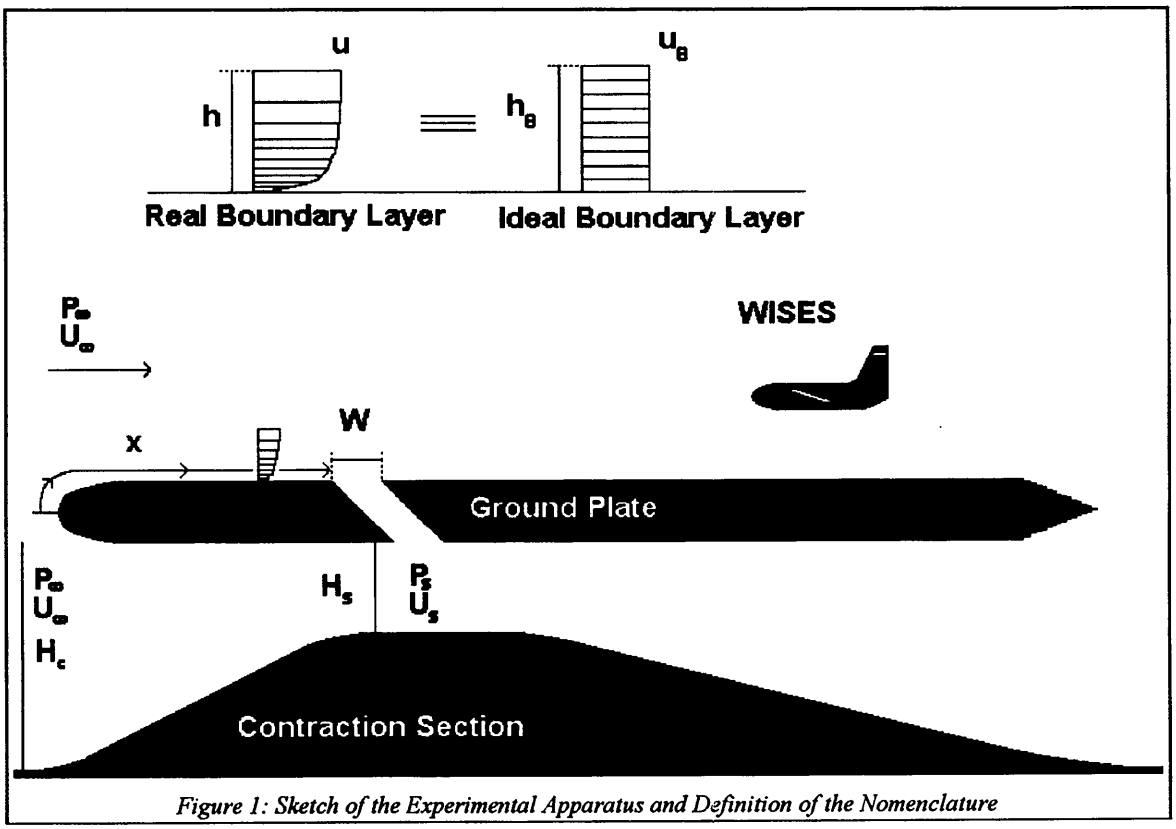

Figure 1: Sketch of the Experimental Apparatus and Definition of the Nomenclature

2.1. Theoretical Analysis

The following is a theoretical derivation for the relevant design parameters. A number of these were fixed in the current work through practicalities involved in using the wind tunnel such as the

clearance of the ground plate, H_C. Figure 1 also shows the nomenclature used in this analysis.

It is assumed that changes in quantities are isentropic and quasi-static allowing the use of mean properties. It is proposed that the momentum of the boundary layer can be expressed in terms of an equivalent momentum velocity, U_θ, and momentum height, h_θ, such that the total momentum of the two layers are the same. This is shown symbolically at the top of Figure 1 where the equivalent boundary layer height and momentum velocity are shown equated to the true boundary layer velocity, U, and height, h. Equating both the mass flow and the momentum of the real and hypothetical boundary layers, we obtain Equation 3 and Equation 4, (L= the slot length);

$$M = \int_0^h \rho L U dy = \int_0^{h_\theta} \rho L U_\theta \, dy$$

$$\Rightarrow \int_0^1 \left(\frac{U}{U_\infty}\right) d\left(\frac{y}{h}\right) = \left(\frac{U_\theta}{U_\infty}\right)\left(\frac{h_\theta}{h}\right) = I_1 \qquad (3)$$

$$\& \; M = \rho L h U_\infty I_1$$

$$\int_0^h \rho L U^2 dy = \int_0^{h_\theta} \rho L U_\theta^2 \, dy$$

$$\Rightarrow \int_0^1 \left(\frac{U}{U_\infty}\right)^2 d\left(\frac{y}{h}\right) = \left(\frac{U_\theta}{U_\infty}\right)^2 \left(\frac{h_\theta}{h}\right) = I_2 \qquad (4)$$

Using Newton's 2nd Law, the pressure difference between above and below the ground plate can be related to the change in momentum of the boundary layer. It is assumed that the whole of the boundary layer passes smoothly through the slot with no component of the free stream*, (W= the slot width);

$$P_S - P_\infty = \frac{F}{A_{SLOT}} = \frac{M\left(U_\theta - U_S\right)}{W L} \qquad (5)$$

If the flow through the ramp section and the flow above the ground plate originate from the same source then Bernoulli's equation can be used to relate the pressure and velocity in the free stream and below the ground plate. This is shown in Equation 6;

$$P_S - P_\infty = \tfrac{1}{2} \rho U_\infty^2 \left[1 - \left(\frac{U_S}{U_\infty}\right)^2\right] \qquad (6)$$

Substituting Equations 3 and 4 into Equation 5, and equating to Equation 6 leads to the quadratic Equation 7 which has the solution given by Equation 8.

* This is almost certainly untrue and probably introduces the most uncertainty into the analysis.

$$\left(\frac{U_S}{U_\infty}\right)^2 - \left(2\frac{h}{W}I_1\right)\left(\frac{U_S}{U_\infty}\right) + \left(2\frac{h}{W}I_2 - 1\right) = 0 \tag{7}$$

$$\left(\frac{U_S}{U_\infty}\right) = \frac{h}{W}I_1 \pm \sqrt{\left(\frac{h}{W}I_1\right)^2 - 2\frac{h}{W}I_2 + 1} \tag{8}$$

Note: The choice of sign in Equation 8 is dependent upon the relative pressures above and below the plate (i.e. the direction of suction). In the current circumstances the positive sign should be used.

From Equation 8 it can be seen that the ratio of the slot width to the boundary layer height plays an important role. In the current work it was decided for simplicity to design the apparatus assuming that the slot width would be the same as the boundary layer height. The effect of changing the slot width from the design conditions could then be found experimentally.

It only remains to evaluate the integrals in Equation 8 in order to find the required velocity ratio. The required height, H_s , can be found using continuity through the contraction including the mass flow through the slot as shown in Equation 9.

$$\begin{aligned} \rho L H_S U_S &= \rho L \int_o^h U dy + \rho L H_C U_\infty \\ \Rightarrow H_S &= \frac{U_\infty}{U_S}\left(hI_1 + H_C\right) \end{aligned} \tag{9}$$

Thus, given the solution to Equation 8 and with prior knowledge of the boundary layer height at the slot (which is also required to set the slot width) then the required height of the ramp can be obtained. It should be noted that both U_S , H_S and W are dependent upon the boundary layer properties at the slot which vary with Reynolds number, free stream turbulence and the surface roughness of the ground plate.

2.2. Theoretical Results with a Laminar and a Turbulent Boundary Layer on the Ground Plate

If the boundary layer on the ground plate is laminar then the Blasius solution for flow on a flat plate can be used with good accuracy. If the boundary layer on the ground plate is turbulent then the 7^{th} Power Law can be used. With design conditions such that the ground plate height, H_C , is 0.567m*, the distance from the leading edge is 1m and the free stream velocity is 10m/s we obtain a local Reynolds number at the slot of 6.84×10^5 which is within the transition region for flow on a flat plate so the boundary layer at the slot is probably transitional or turbulent.

* This height was determined by practicalities of installing the apparatus.

Table 2 and Figure 2 give the results of calculations of the required contraction ratio, H_S/H_C , for both boundary layer types and the results show that the ratio is broadly similar for both types of boundary layer (consider the vertical scale) but in detail the turbulent case requires more suction than the laminar case as might be expected. At low clearances the Reynolds number effect is greatest but as the clearance increases the effect decreases and the contraction ratio becomes essentially constant for a given boundary layer type.

Table 2 : Theoretical Calculations of the Suction Parameters

	Laminar Boundary Layer (Blasius)	Turbulent Boundary Layer ($1/7^{th}$ Power Law)
I_1	0.66	0.88
I_2	0.52	0.78
h / h_θ	1.22	1.02
U_θ / U	0.8	0.89
U_S / U	1.28	1.33
h / mm	6.04	25.18
H_S / mm	447.48	441.78
H_S / H_C	0.789	0.779

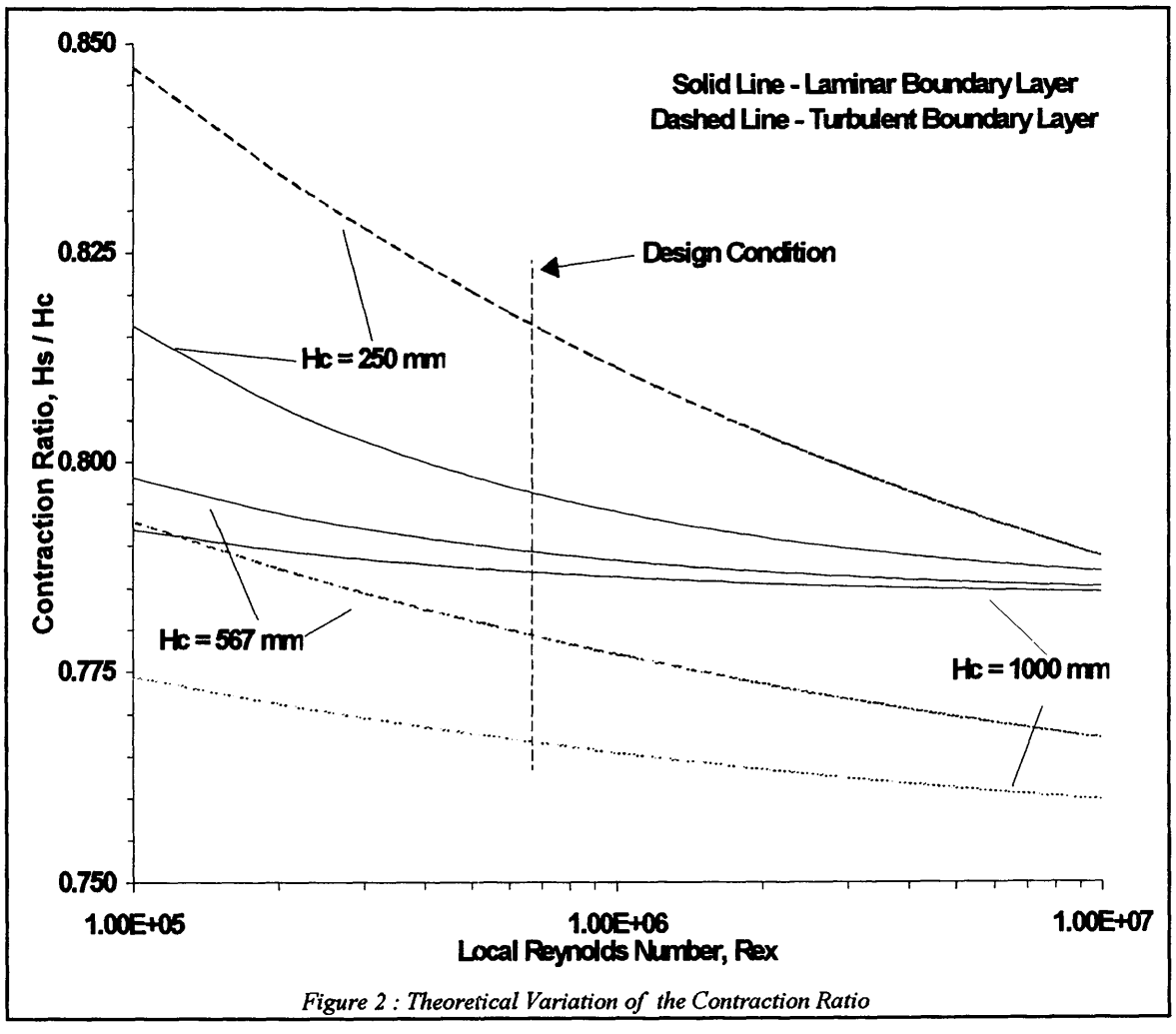

Figure 2 : Theoretical Variation of the Contraction Ratio

3. Experimental Techniques and Uncertainties

The wind tunnel was a closed return type with working section dimensions of 3 m × 2 m × 15 m (width × height × length). The free stream turbulence intensity was generally less than 0.34% and the free stream velocity could be controlled to within 0.1 m/s.

3.1. Ground Plate Apparatus

Figure 3 shows the principle dimensions of the ground plate and contraction section. The original 45 degree leading edge is marked although this was replaced by an elliptical leading edge as discussed in Section 4.1. It was decided that two ramps should be built to provide the suction force which had 30% lower and higher contraction ratio's than the design case (see Table 2). The specific ramp dimensions are given in Table 3.

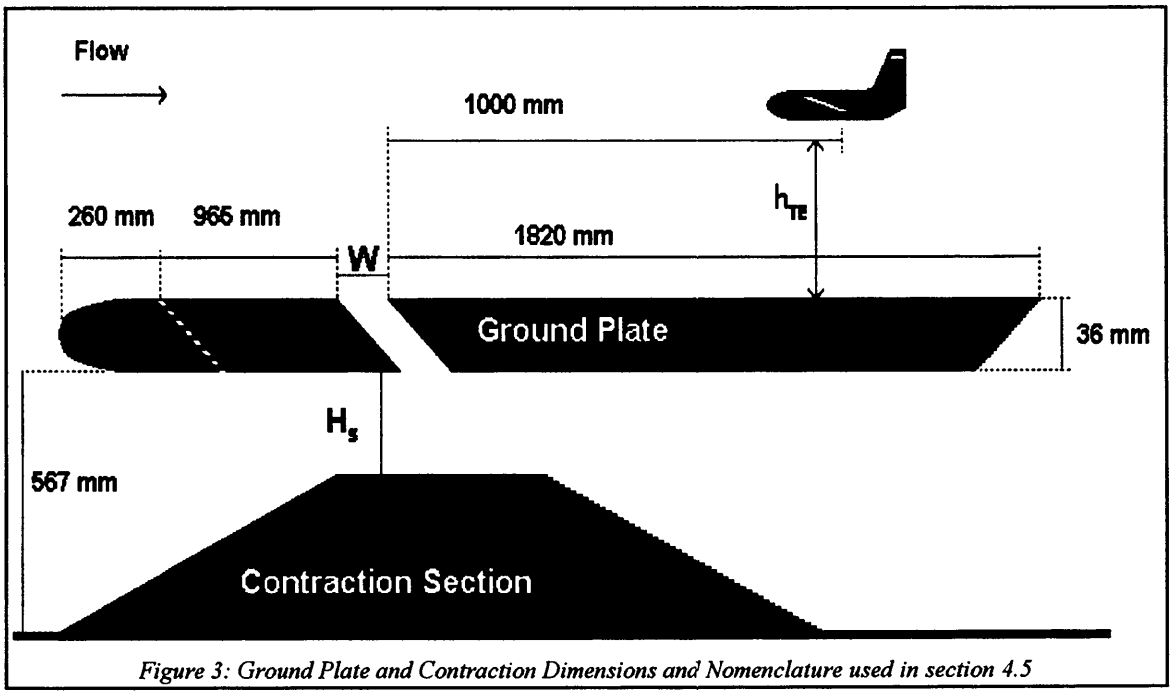

Figure 3: Ground Plate and Contraction Dimensions and Nomenclature used in section 4.5

Table 3 : Ramp Dimensions

	Low Suction	High Suction
H_C / mm	567	567
H_S / mm	482	412
H_S / H_C	0.85	0.73

Installation of the ramps was very easy and it only took approximately twenty minutes to replace either ramp. Unfortunately the upper surface of the ground plate bowed downwards slightly under its own weight so that when the slot was open the theory did not truly represent the physical situation. This was remedied by installing two jacks between the ramp and the lower surface of the ground plate. The effect of the extra blockage and interference caused by the presence of the jacks could not be accurately discerned. This problem was remedied without the use of jacks for the tests with the contoured slot (see section 4.3.4) by modifications to the structure of the ground plate.

Due to the large width of the ground plate (3m) extra strength was required to bear the weight of the apparatus and personnel. This was provided by two vertical plates which were secured to the original floor and the lower side of the ground plate. These supports probably produced negligible interference effects but meant that only the central section was fitted with a ramp. The difference between the sections with and without a ramp was extremely large and this defect should be corrected for future experiments particularly for models with large wing spans.

3.2. Velocity Measurements

The dynamic pressure was measured by a pitot-static tube via a sensitive pressure transducer which was read by an analogue to digital processing card in a PC. The digital signal was then averaged after the tests had taken place and converted to velocity measurements.

The probe height from the ground plane was initially set with the wind-tunnel switched off. When the airflow was switched on the probe and traversing apparatus may have bent in an unknown direction and by an unknown amount so the true height from the ground plane, y, could not be taken directly from the experimental values. Instead the height was obtained from the velocity data by two methods. The first was by extrapolating the data to the local velocity, u=0 line which should correspond to the origin and was the least accurate method. The second method was only possible when the measured velocity became constant at low heights indicating that the pitot-tube was resting on the ground plane and actually measuring the velocity at a constant height. This was the most accurate method available.

The outer flow reference velocity, U, was also obtained by two methods. When a small amount of data was available in the outer flow, the maximum measured velocity was used. This was the least accurate method. When a large amount of data was available, an average of the readings was used. This is much more accurate and the average was typically taken from a sample size of 500. The boundary layer heights, h, corresponded to a local velocity, u, of 99% of the outer flow reference velocity.

The uncertainty of the results was assessed using the method of S.J. Kline & F.A. MCClintock - 1953 [6] which attempts to account for the propagation of uncertainties within calculations involving single sample data sets. The ranges indicated in subsequent figures are based on the experimental uncertainties shown in Table 4.

Table 4 : Experimental Uncertainties

Quantity	Uncertainty (≅ 95% confidence)
u	± 0.2 m/s
U (Maximum)	± 0.25 m/s
U (Average)	± 0.2 m/s
y (1 mm Pitot-tube)	± 0.5 mm
y (9 mm Pitot-tube)	± 4.5 mm
h (Extrapolated)	± 2.5 mm
h (Constant u)	± 1 mm

The pitot-tube could be traversed either in discrete steps at the discretion of the user (stepwise) or

automatically with a time delay at each step (continuous) during which data was obtained. In order to test the techniques, boundary layer profiles obtained by both traversing methods and the results are compared in Figure 4. The results are within the uncertainty intervals of each test (only one set of intervals is shown for clarity) and it is concluded that both techniques are reliable.

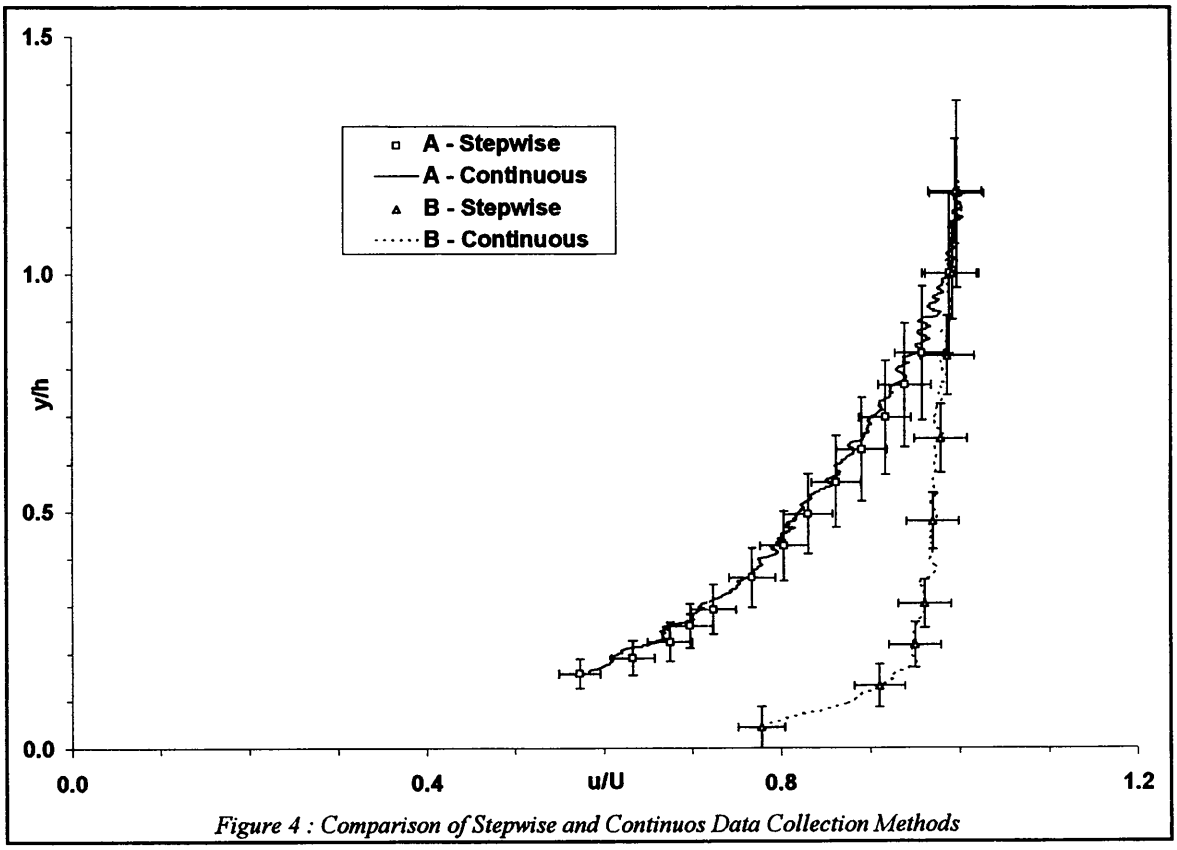

Figure 4 : Comparison of Stepwise and Continuos Data Collection Methods

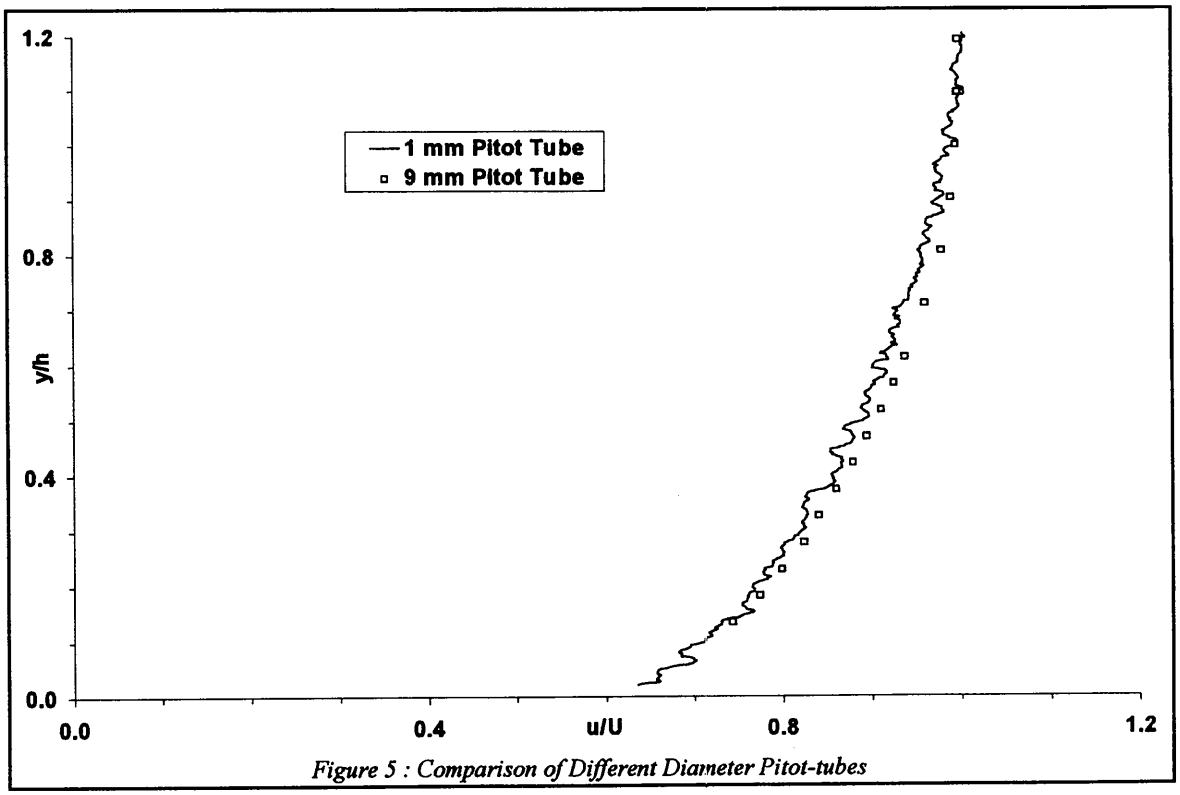

Figure 5 : Comparison of Different Diameter Pitot-tubes

A further potential problem with measurements of low velocity using pitot-tubes is the interference of viscous effects at low Reynolds numbers (based on the tube outer diameter) as discussed by D.W. Bryer & A.A. Pankhurst - 1971[7]. For the two pitot-tube diameters used in this study, the local Reynolds numbers being measured were at least a factor of 4 greater than the lower limit which is dependent upon the turbulence levels and the shape of the pitot-tube but is generally of the order of 100.

The extent of any interference effects may be considered small given that no visible effects due to a 9 fold increase in tube diameter could be seen as shown in Figure 5 for the two pitot-tubes under similar experimental conditions

3.3. Flow Visualization Techniques

A standard oil vaporizer was used to produce smoke filaments via a hand held probe(developed at the National Physics Laboratory, UK). However, the filaments were very dispersed and erratic and it is the authors opinion that the oil pump was not sufficiently smooth and should be replaced before further experimentation. The probe was generally placed near the leading edge at various heights both above and below the ground plate. A video camera was used to record the smoke flow and photographs were obtained from the video recording or during the experiment.

A surface-oil visualization technique was also used where a mixture of an oil, a pigment (which will show up against the surface) and a dispersant was applied over the required area. The relative mixtures were obtained through a limited amount of trial and error. Once the pattern had formed the tunnel was switched off and the results easily photographed. Extremely informative results can be obtained from use of a fluorescent pigment where the results are photographed in ultraviolet light on black and white film.

A theoretical and general application guide to this method is presented by R.L. Maltby - 1962 [8] and W. Merzkirch - 1987 [9]. For air flows it is usual to use a liquid which has low viscosity and which ideally evaporates after a short time (sufficient for the pattern to form). This was not possible in the current tests and a rather thick oil had to be used. It was obvious that the mixture was too viscous and probably formed a deep layer which altered the boundary conditions at the surface. However, the results are considered useful on a qualitative basis and can indicate some of the larger scale flow features. Extreme care should be taken when trying to infer detailed information from these results.

4. Discussion of the Experimental Results

The experiments were conducted at an average free stream speed of 10.7 m/s corresponding to a free stream Reynolds number of 7.33 $\times 10^5$ /m. The velocity profiles within the boundary layer were measured by the techniques described in Section 3.2. The ground plate dimensions are shown in Figure 3 (see Section 3.1). Limitations to the traversing mechanism did not allow measurements further upstream than 150 mm downstream of the slot.

4.1. Effect of Different Leading Edges (Without Suction)

Measurements without suction (i.e. with the slot closed) were taken in order to allow accurate comparisons when suction was used. In addition, initial refinement of the basic ground plate apparatus could be carried out.

The ground plate originally had a leading edge cut at 45 degrees to the free stream direction with a front plate length of 965 mm (see Figure 3). The velocities within the boundary layer on the ground plate are shown in Figure 6 and have been non-dimensionalised by the appropriate quantities. The Blasius and $1/7^{th}$ power law profiles have also been plotted for comparison. The profiles show that the layer was turbulent and the self similarity suggests fully developed flow conditions.

The layer was very large (of the order of 70 mm) and needed to be reduced in order to give the suction a chance of working. A reduction of approximately 50% at each measuring position is shown in Table 5 and was achieved by adding an elliptical section (2:1) onto the sharp leading edge (increasing the front plate length by 260 mm).

Table 5 : Initial Boundary Layer Height, h / mm.

Measuring Position (From the Slot)	Sharp Leading Edge	Elliptical Leading Edge
150 mm	62.5	29.6
550 mm	74.5	33.5
1000 mm	76.9	39.0

The subsequent velocity profiles are shown in Figure 7. The shape of the profiles and the lack of self-similarity suggests transition to turbulence was occurring which is also supported by the intermediate variation of the boundary layer height with local Reynolds number (measured from the leading edge) as shown in Figure 8 for both the sharp and elliptical leading edges. Given the insensitivity of the theory to the state of the boundary layer (see Figure 2) it was thought that a transitional boundary layer in the region of the slot would have little effect on the effectiveness of the technique.

The data in Figure 8 for the sharp leading edge shows boundary layer heights that would be associated with 2.5 times the actual Reynolds numbers; this is thought to be due to a separation bubble originating at the sharp leading edge which is especially likely if the ground plate was at a positive incidence to the free stream flow although this has not been confirmed.

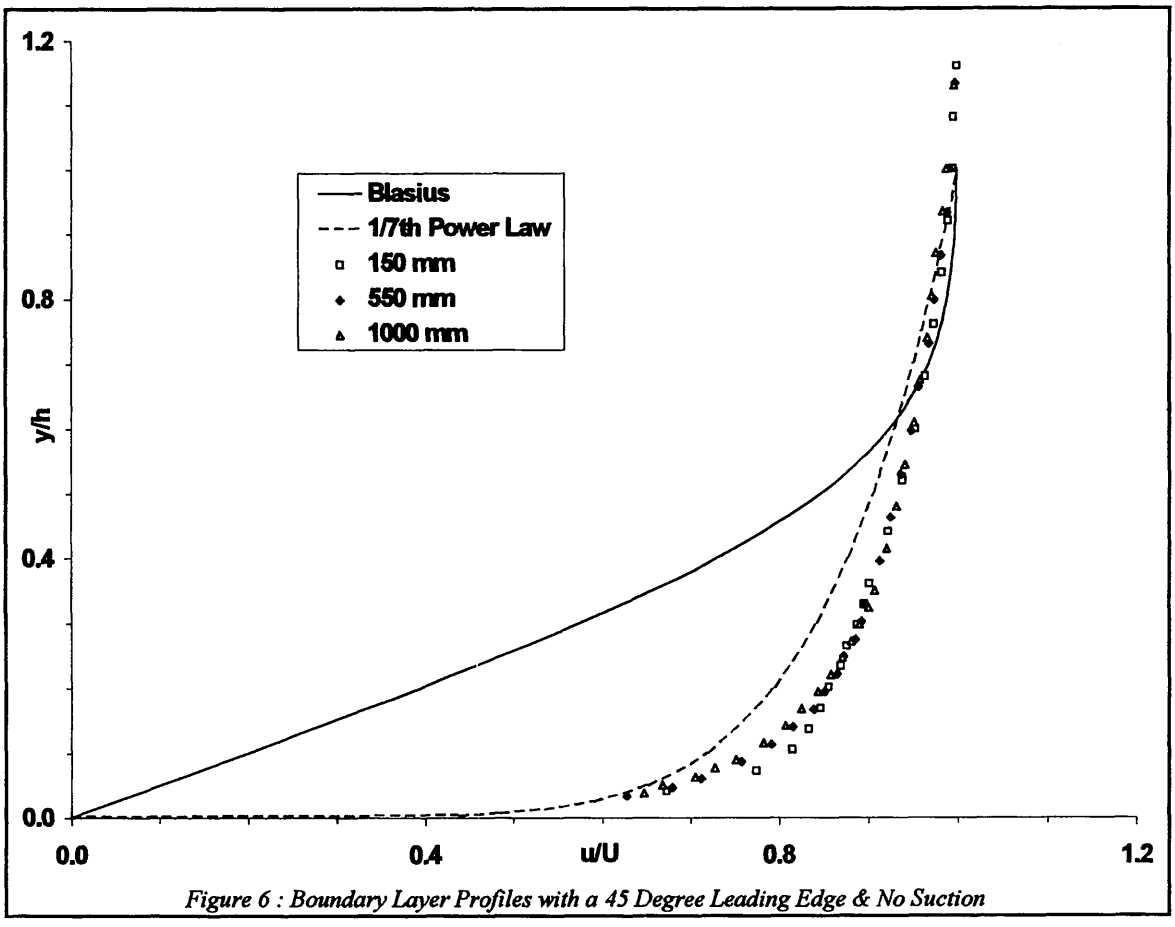

Figure 6 : Boundary Layer Profiles with a 45 Degree Leading Edge & No Suction

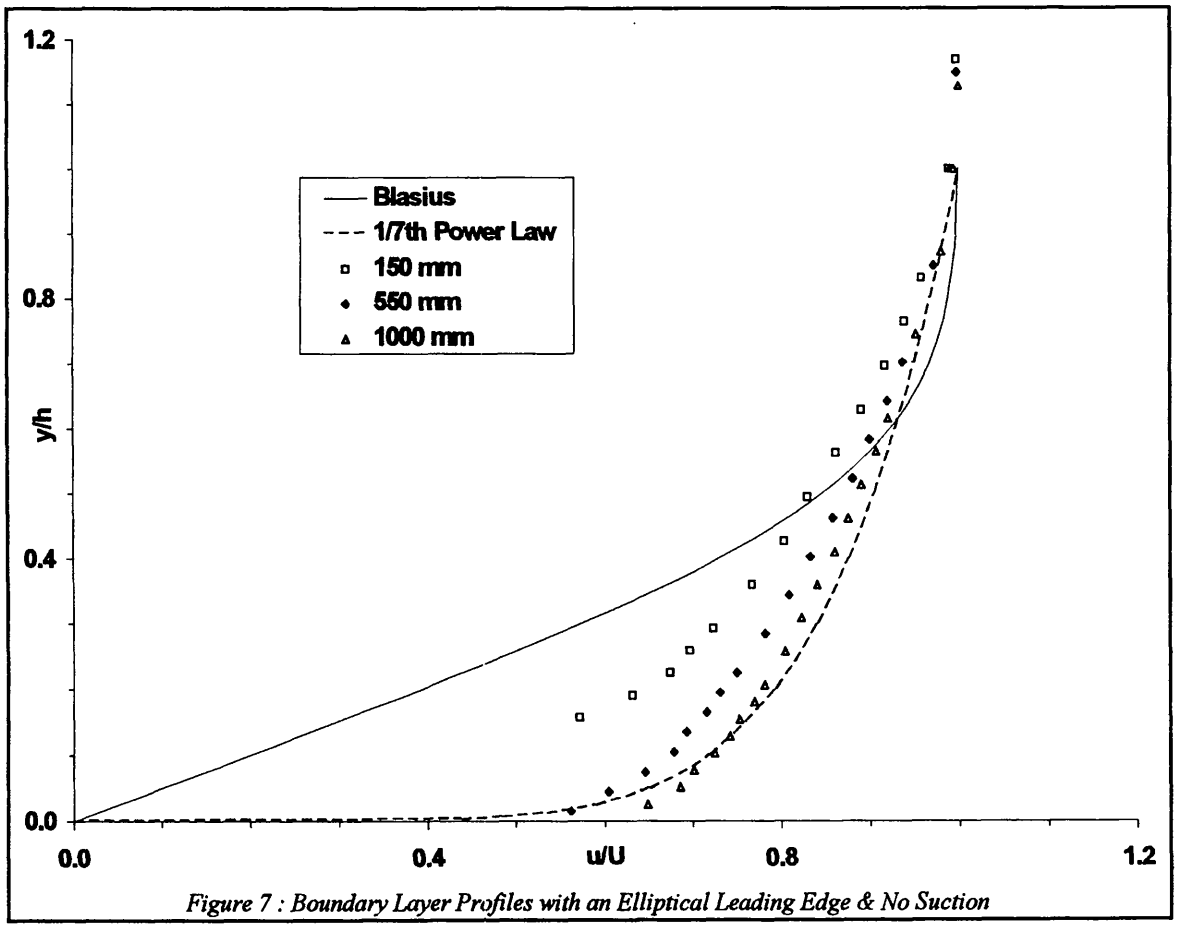

Figure 7 : Boundary Layer Profiles with an Elliptical Leading Edge & No Suction

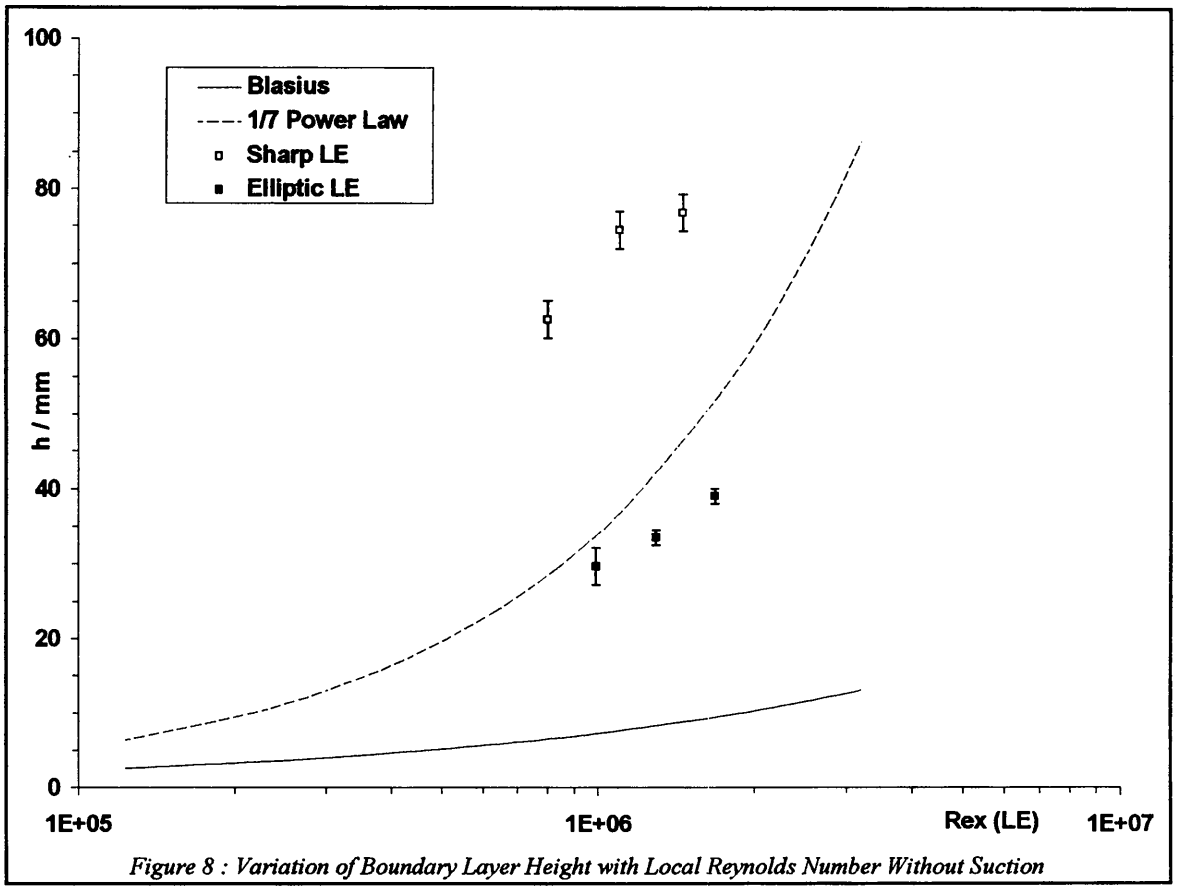

Figure 8 : Variation of Boundary Layer Height with Local Reynolds Number Without Suction

The almost constant variation between the actual and semi-empirical profiles on Figure 8 for the elliptical leading edge can be used to approximate the effective transition point of the boundary layer which is estimated to be 326 mm from the leading edge. Thus the flow over the slot was probably turbulent and the height of the boundary layer at the slot can be estimated to be 26 mm (from a Reynolds number of 8.5×10^5). It must be stated that the procedure for finding the effective transition point is not very accurate and should be used as a rough guide only.

The effectiveness of the elliptical leading edge meant that it was used in all subsequent experiments.

4.2. Phenomenological Effects of Introducing Suction

The flow field near the slot was visualized as described in Section 3.3. The techniques were not entirely satisfactory but they did allow some features of the flow field to be observed.

The general effect of suction on the boundary layer was clearly visible through the use of the smoke filaments. Without suction the boundary layer was observed to grow rapidly whilst with suction the layer was almost entirely removed and the downstream boundary layer grew slowly. Detailed analysis of the flow revealed a number of problems but the apparatus was a success in terms of reducing the boundary layer height down stream of the slot.

Plate 1 : Surface-Oil Patterns in the Region of the Slot

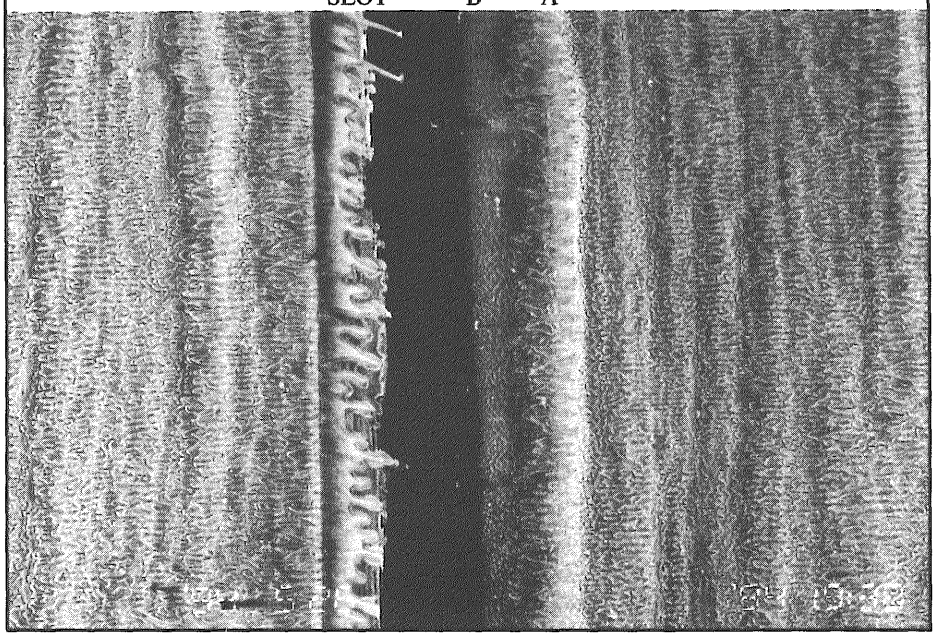

Plate 1 shows the results of a surface-oil test with flow from left to right. The flow on the sloping surface in the slot illustrates a problem with this type of visualization, namely the flow of the mixture under gravity. This can be avoided by applying only a very thin mixture on the slope and the upstream surface and/or by use of a solvent which evaporates over a relatively short time. Vast improvement in the definition of the results can also be obtained using this method.

Just downstream of the slot the oil has been swept along by the high speed free stream flow which comes into contact with the plate after the boundary layer has been removed. This process is the cause of the build up of oil further downstream (point A) which may also have been avoided using an evaporating solvent. The origin of the new boundary layer (point B) can be inferred from the point where the oil patterns are less coarse corresponding to the lower surface shear stress associated with a laminar layer.

Plate 2 : Smoke Flow Through The Slot

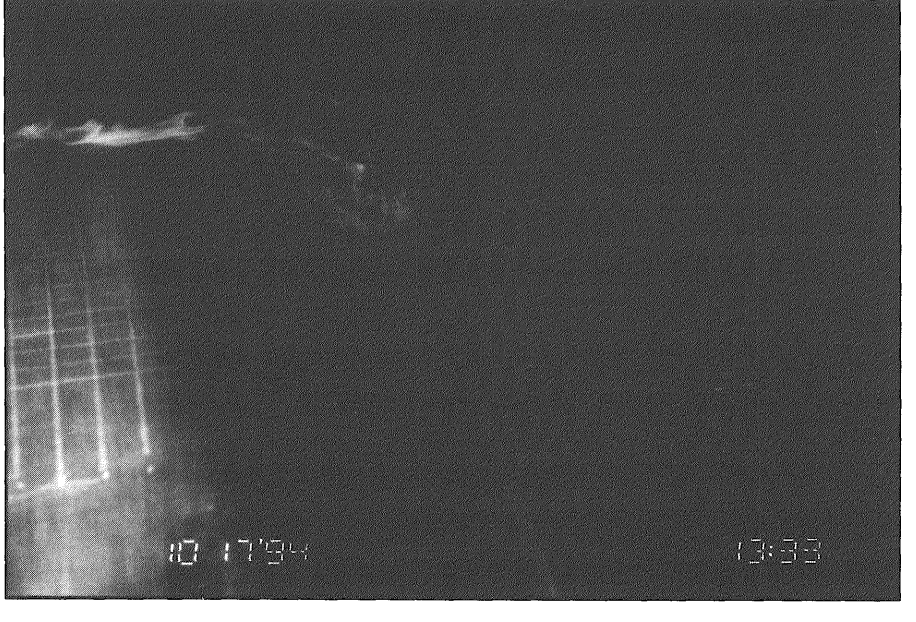

Plate 2 shows the flow of smoke through the slot (from left to right). Although no details are visible some important general features can be seen.

An important flow separation and recirculation feature can be seen in the slot. The surface smoke stream separates at the upstream edge of the slot and then moves into the slot. Below this stream a recirculating region was visible but could not be

easily captured on film due to the irregular influx of smoke into the region and the speed at which the smoke then flowed through the slot. The separation was not temporally nor spatially steady and it effectively reduced the width of the slot. Also the stagnation point on the downstream section of the slot (probably near the upper edge) would be unsteady which could cause disturbances in the flow over the upper surface and promote transition and hence increase the growth rate of the boundary layer.

In an attempt to reduce the separation effects in the region of the slot, the edges of the slot were contoured and this is discussed in Section 4.3.4.

4.3. Discussion in Terms of Boundary Layer Heights

The reduction of the height of the boundary layer on the ground plate was the prime objective of designing the suction apparatus and as such this shall be discussed first with respect to introduction of the suction apparatus and then with respect to changes in the level of suction, slot width and slot shape.

4.3.1. Effect of Introducing Suction

The introduction of suction reduced the heights of the boundary layer on the ground plate by approximately 50% as shown in Table 6 and in this sense the apparatus can be considered successful.

Table 6 : Effect of Suction on the Boundary Layer Height, h / mm.

Measuring Position (From the Slot)	No Suction	With Suction
150 mm	29.64	11.65
550 mm	33.5	18.4
1000 mm	39	23.25

4.3.2. Effect of Changing the Level of Suction

As was described in Section 3.1, two ramp sections were built to allow different suction levels to be tested. Figure 9 shows the variation of the boundary layer height with local Reynolds number (measured from the slot) for the different levels of suction with a 45 degree slot of width 40 mm.

The theory described in Sections 2.1 and 2.2 predicted that changes in the level of suction would have little effect on the performance of the apparatus, however, small improvements can be seen in Figure 9 given the experimental uncertainties. This is generally encouraging for the technique as a whole and is acceptable given the simplicity of the theory.

4.3.3. Effect of Changing the Slot Width

The effects of increasing the slot width from 20 mm to 40 mm with a constant (low) level of suction is shown in Figure 10. The theory indicated that increasing the width of the slot would require less suction, so increasing the slot width, with a constant level of suction, should have improved the performance (greater suction was present than required). The small improvement observed was within the experimental uncertainty in general. This may have been due to flow separation from the upstream edge of the slot which effectively reduced the slot width. Also, the effects of too much suction may not be as

simple as the model suggests, particularly in relation to the external flow.

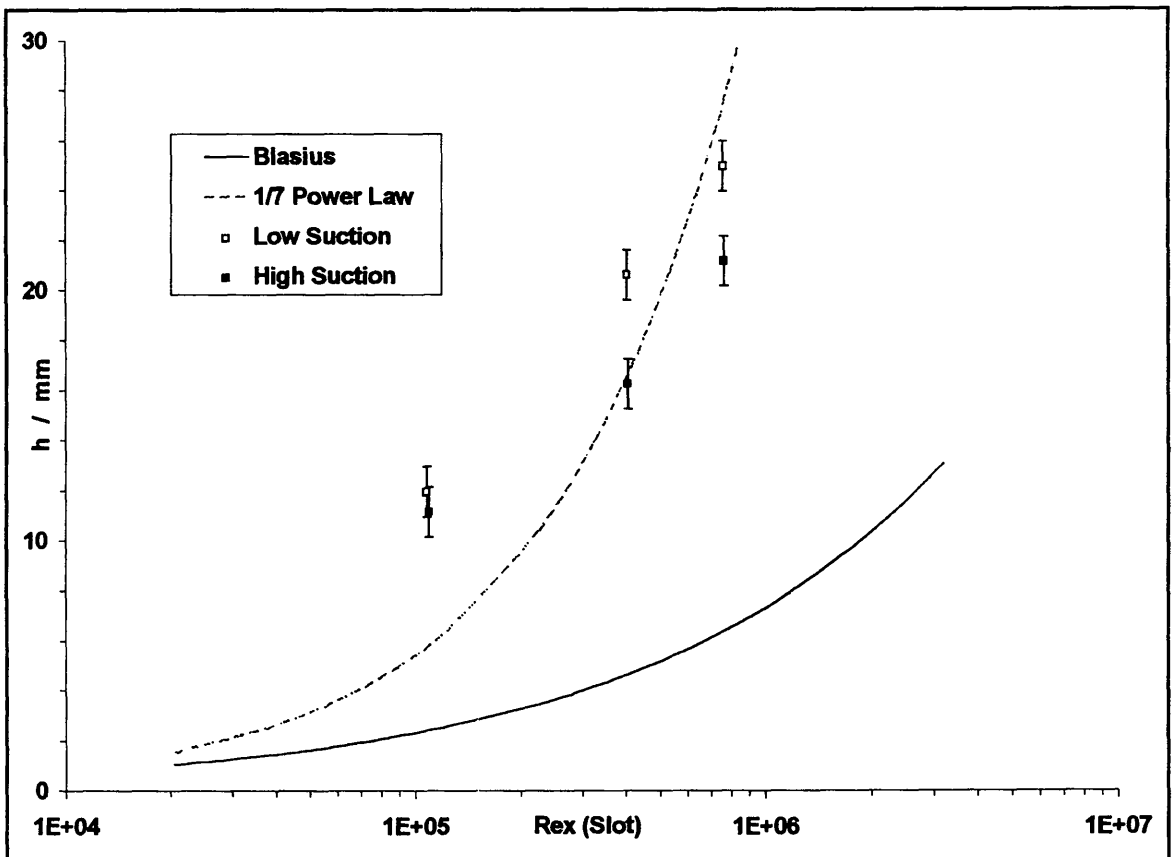

Figure 9 : Variation of Boundary Layer Height with Local Reynolds Number Due to Changes in the Level of Suction

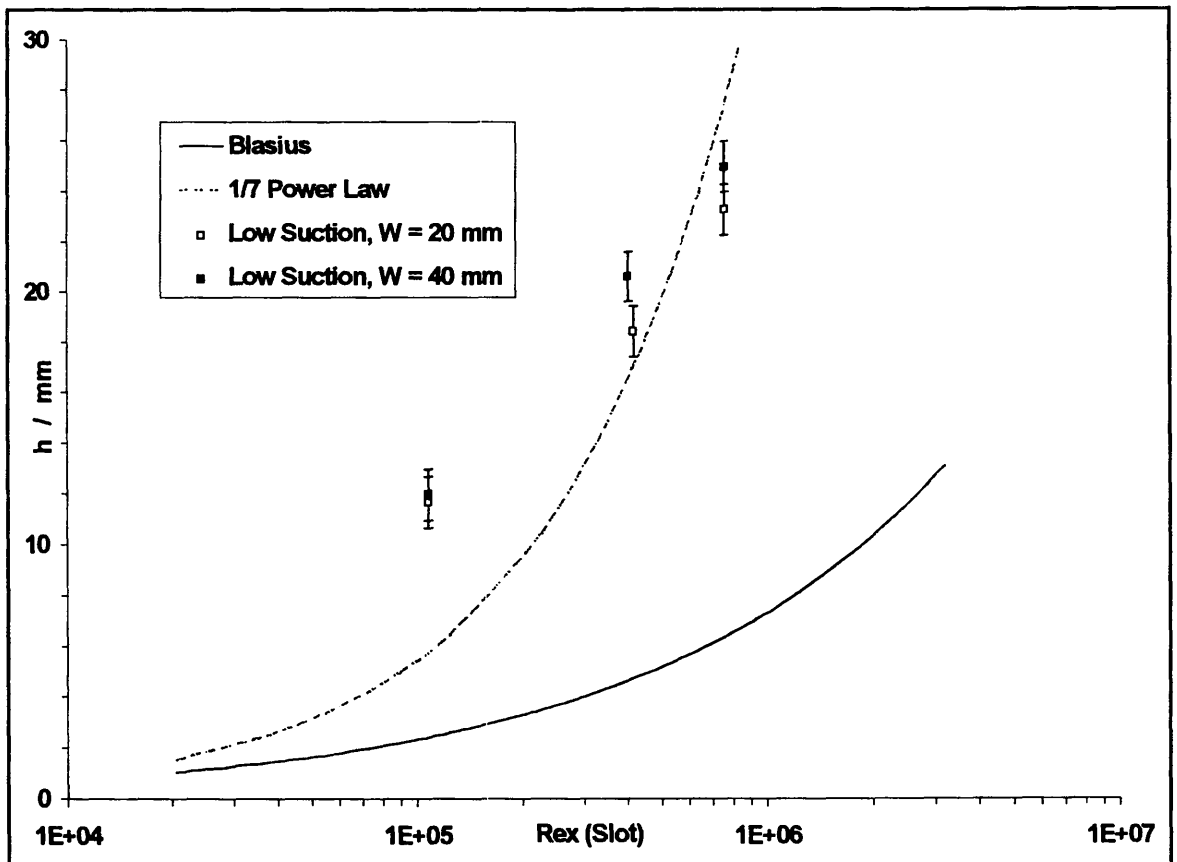

(70) *Figure 10 : Variation of Boundary Layer Height with Local Reynolds Number Due to Changes in the Slot Width*

4.3.4. Effect of Changing the Slot Shape

In an attempt to reduce the separation effects in the region of the slot, the edges of the slot were contoured as shown in Figure 11. The upstream edge was shaped so as to have a maximum change in elevation of 3.5 degrees per mm. This was in order to reduce the severity of the flow separation. The downstream edge was shaped to provide a smooth interface between the slot and the downstream flow.

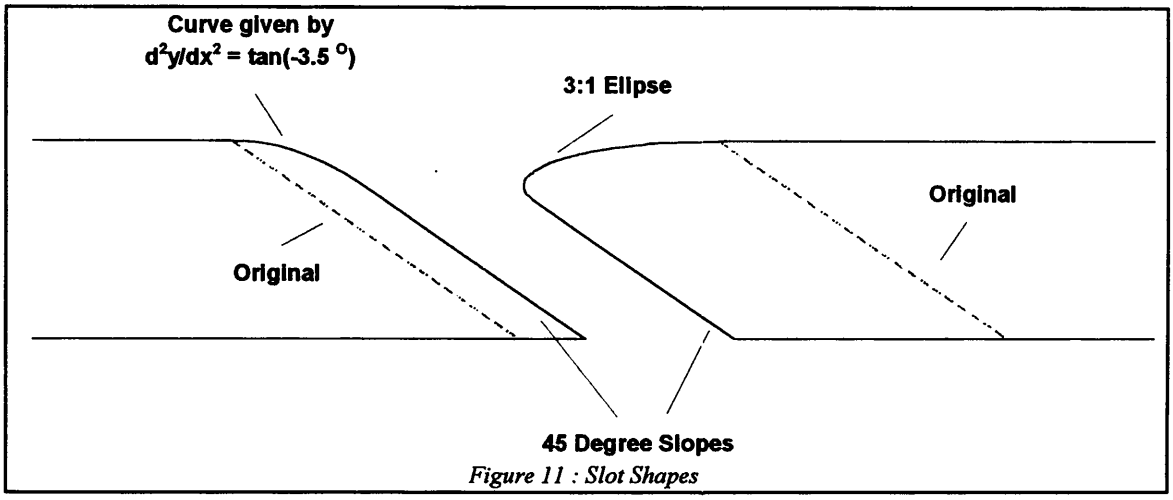

Figure 11 : Slot Shapes

Figure 12 shows the effect of changing the shape of the slot with a constant level of suction (high) and slot width (40 mm). The changes were generally within the experimental uncertainties but the growth rate was slightly improved which is probably due to increased stability of the downstream boundary layer due to the smooth downstream edge of the slot and the reduction in movement of the stagnation point.

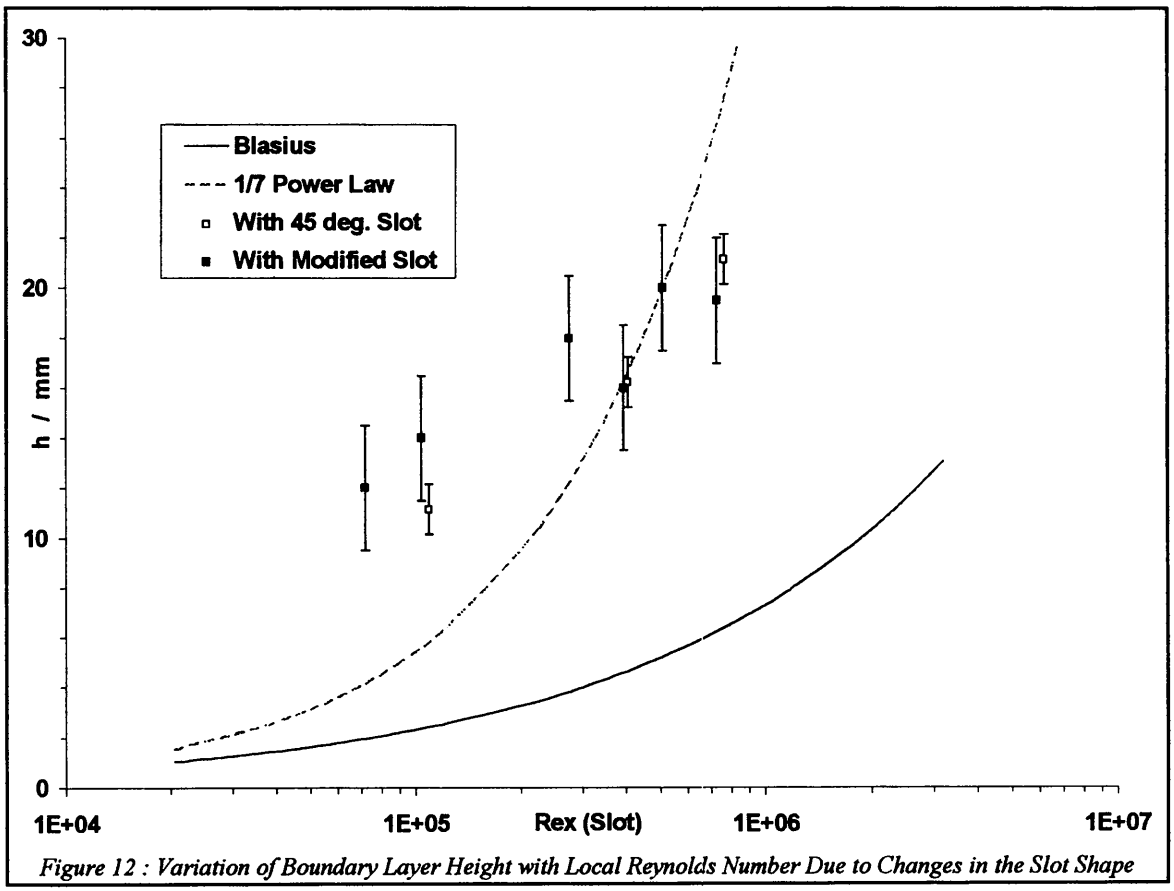

Figure 12 : Variation of Boundary Layer Height with Local Reynolds Number Due to Changes in the Slot Shape

4.4. Discussion in Terms of Velocity Profiles

Figure 13, Figure 14 & Figure 15 show the velocity profiles in the boundary layer down stream of the slot at each measuring position for the different experimental configurations. The profiles have been non-dimensionalised by the appropriate quantities and the Blasius and $1/7^{th}$ power law profiles are plotted for comparison.

At 150 mm downstream from the slot (Figure 13) the effect of the addition of suction is large and the momentum deficit of the boundary layer is greatly reduced. The increase in the level of suction and addition of the contoured slot produces a further small improvement.

At 550 and 1000 mm downstream from the slot (Figure 14 & Figure 15) the profiles are very similar whatever the experimental configuration and fall very close to the $1/7^{th}$ power distribution suggesting fully turbulent flow conditions. Modification of the slot did not have the desired effect in terms of delaying the transition to turbulence.

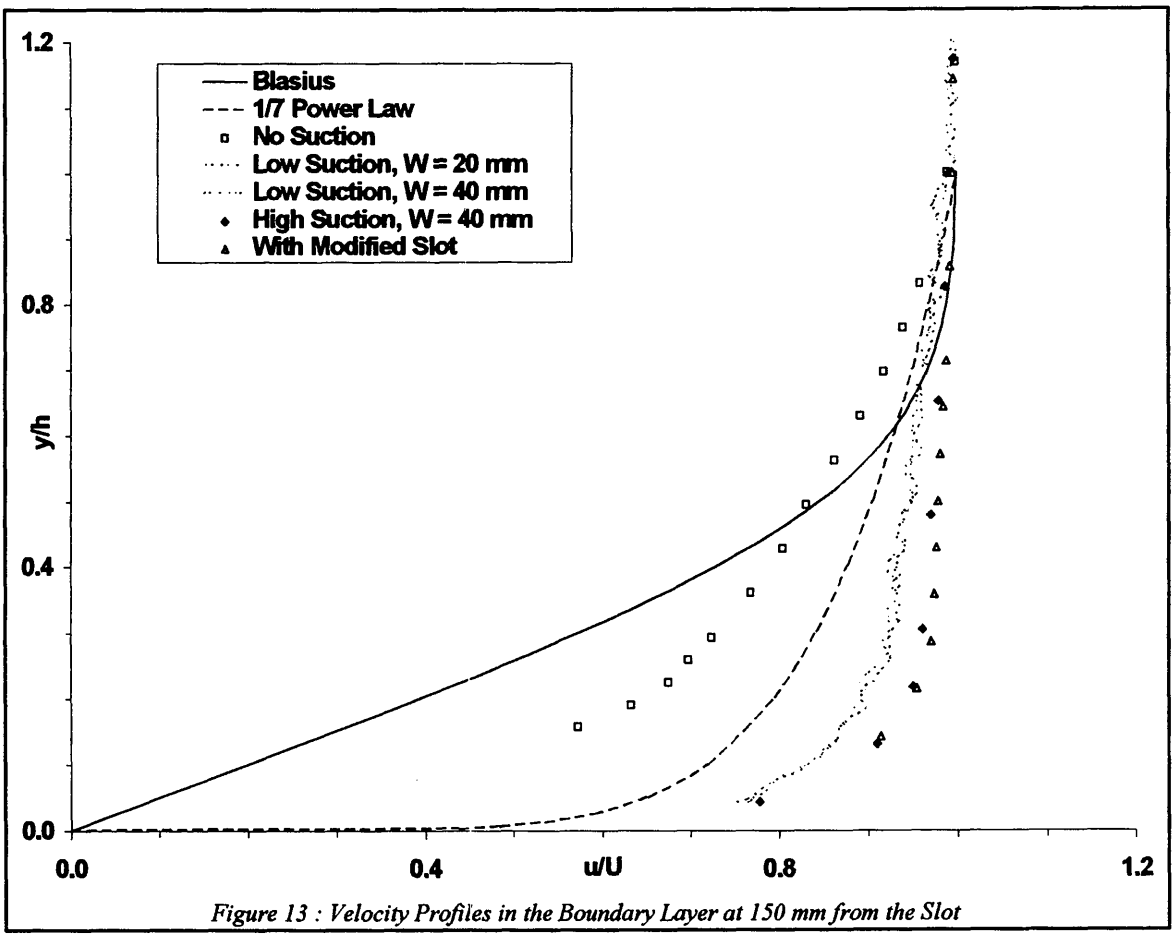

Figure 13 : Velocity Profiles in the Boundary Layer at 150 mm from the Slot